ELSEVIER

Ceramics International 33 (2007) 463–469

CERAMICS INTERNATIONAL

www.elsevier.com/locate/ceramint

Effect of ZrO_2 nucleant on crystallisation behaviour, microstructure and magnetic properties of $BaO–Fe_2O_3–B_2O_3–SiO_2$ glass ceramics

M. Mirkazemi [a], V.K. Marghussian [a,*], A. Beitollahi [a], S.X. Dou [b], D. Wexler [c], K. Konstantinov [b]

[a] *Ceramics Division, Department of Materials, Iran University of Science and Technology, Narmak, Tehran 16844, Iran*
[b] *Institute of Superconducting and Electronic Materials University of Wollongong, NSW 2522, Australia*
[c] *School of Materials and Mechanical Engineering, Wollongong University, Wollongong, NSW 2522, Australia*

Received 29 July 2005; received in revised form 22 August 2005; accepted 27 October 2005
Available online 20 January 2006

Abstract

Differential thermal analysis, X-ray diffractometry and scanning electron microscopy with energy dispersive spectroscopy were used to study the crystallisation of glass ribbons with a composition of 35% BaO, 35% Fe_2O_3, 20% B_2O_3 and 10% SiO_2 (mol%) with 1% ZrO_2 added as a nucleant. The magnetic properties of ribbons prepared via cooling the melts between steel rollers were measured with a vibrating sample magnetometer.

The addition of ZrO_2 apparently resulted in a quite distinct glass-in glass phase separation in as prepared specimens, greatly affecting the nucleation process.

Heat treatment of specimens at their DTA exo-peak temperature of 721 °C led to the formation of $BaFe_{12}O_{19}$ and BaB_2O_4 as the only crystalline phases. The glass ribbons heat treated in one-stage exhibited a quite non-uniform distribution of particles exhibiting exagerated grain growth, while a two-stage heat treatment at 526 and 721 °C for different time periods generally led to more uniform distribution of platelet particles. The values of saturation magnetisation of specimens were in the M_s = 23–29 emu/g range, while the coercivity values varied between H_c = 1800–3000 Oe.

Keywords: C. Magnetic propertirs; D. Glass ceramics; E. Hard magnets; $SiO_2–B_2O_3–Fe_2O_3–ZrO_2$; Ferrites

1. Introduction

The glass crystallisation method has been widely used to synthesise various magnetic materials, especially barium hexaferrites, in recent years.

Barium hexaferrites owing to their superior properties have been utilised in various applications as permanent magnets and particulate media for recording high density information. Most investigators have chosen B_2O_3 as a glass former for their base glass compositions which are mainly located in the $BaO–Fe_2O_3–B_2O_3$ system. Many aspects of the process, including the effect of composition, nucleating agents and heat treatment schedule upon magnetic properties have been reported [1–15].

Borate glass offers many advantages in this process, especially for manufacturing particulate recording media, where the amorphous phase must be leached out and the inherent low chemical durability of borate glasses facilitate the process. However, for other applications, e.g. thin films, where the magnetic phase should be dispersed in a glassy matrix, the glass should be chemically more resistant and not vulnerable to moisture attack. There have been some attempts to change the properties of matrix glasses by partially replacing B_2O_3 by other oxides or by application of different glass forming systems [9,10,12–18]. The present authors have shown [13] that it is possible to replace B_2O_3 by 10 mol% SiO_2 in the composition 0.45 BaO·0.25 Fe_2O_3· 0.30 B_2O_3. It was supposed that in addition to improve the durability of glass, this could also decrease the crystallisation rate of the melt and make it more controlable. However, it was proved that the resultant glass ceramics while showing a relatively high coercivity exhibited a low value of saturation magnetisation. In order to increase the values of saturation magnetisation, it was attempted to increase the content of Fe_2O_3 to 35 mol% at the expense of BaO [14]. The above mentioned specimens,

* Corresponding author. Tel.: +98 21 7459151; fax: +98 21 7454057.
E-mail address: v_k_marghus@yahoo.com (V.K. Marghussian).

0272-8842/$32.00
doi:10.1016/j.ceramint.2005.10.011

although exhibited much improved values of M_s but generally showed mostly non-uniform and not quite the expected fine microstructures. In order to improve this, it was decided to add some novel nucleants to the main glass composition. Some aspects of the addition of ZrO_2 as a nucleating agent has been discussed elsewhere [15].

In this paper a more comprehensive account of the addition of ZrO_2 to these glasses has been given with an emphasis on the microstructural changes and their effect on the magnetic properties.

2. Experimental procedure

The glass ribbons with a composition of 35% BaO, 35% Fe_2O_3, 20% B_2O_3 and 10% SiO_2 with addition of 1% ZrO_2 (mol%) were prepared by melting the required amounts of reagent grade chemicals ($BaCO_3$, H_3BO_3, Fe_2O_3 and a very pure quartz sand) in alumina crucibles at 1300–1460 °C for 1 h in an electrically heated furnace. In order to prevent the crystallisation of the high iron glasses the melts were quenched between two steel rollers.

Using this process ribbon samples of ~70 μm in thickness were obtained.

To verify the amorphous nature of the samples they were analyzed by X-ray diffractometry (XRD) (Philips model PW3710 using Co Kα radiation).

Differential thermal analysis (DTA) (Stanton Redcraft model STA-780 & setaram 18–92, 1750 °C) was utilised to determine the glass transition temperature (T_g), dilatometric softening point (T_d) and crystallisation temperature (T_c) of the glass samples. The heating rate was 20 °C min^{-1} and alumina was used as an inert reference material. The shifts of crystallisation (exothermic) peaks (ΔT values) upon changling the DTA sample particle sizes in the <53 μm to the 0.5–0.6 mm range were also measured. The particle sizes were determined utilizing standard sieves.

The samples were then heat treated at their corresponding crystallisation temperatures for different time periods and the crystalline phases developed after heat treatment were identified by XRD. The microstructures were observed with a scanning electron microscope (Cambridge SEM model 360 & Leica Cambrige stereoscan S 440). To prepare the SEM specimens the ribbons were directly etched in 0.5% HF solution for 2.5 min without polishing. The specimens were coated with a thin film of gold prior to the microstructural examinations. The saturation magnetisation (M_s) and coercivity (H_c) values were determined with a vibrating sample magnetometer.

3. Results and discussion

3.1. Differential thermal analysis and crystallisation products

As the DTA traces shown in Fig. 1 indicates the sample having a coarse particle size exhibited an exothermic peak at 721 °C, whereas the specimen with a finer particle size presented an exothermal effect at 715 °C. The relatively small

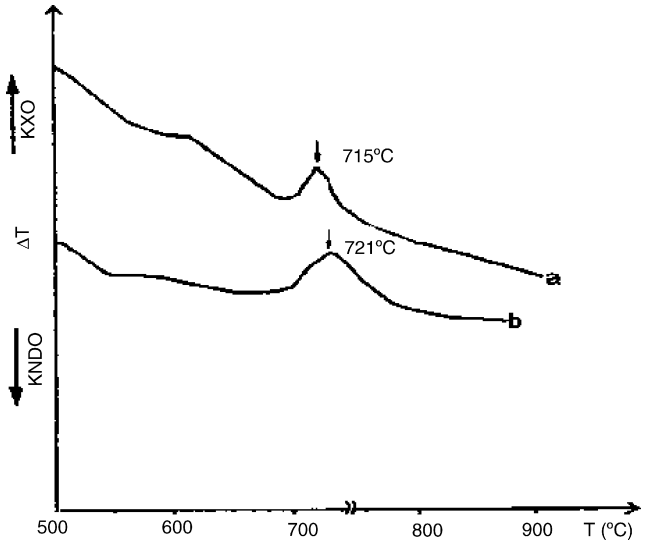

Fig. 1. DTA traces for specimens (a) with fine particle size (<53 μm) and (b) coarse particle size (0.5–0.6 mm).

Table 1
Characteristic temperutures of glass specimens (°C)

Sample	T_g	T_d	T_c
Without ZrO_2 (coarse)	505	534	722
Without ZrO_2 (fine)	505	534	702
With ZrO_2 (coarse)	511	540	721
With ZrO_2 (fine)	511	540	715

DTA peak shift of the fine and coarse particle size specimens ($\Delta T = 6$ °C) can be taken as an indication of the ability of specimens for bulk crystallisation (this shift was 20 °C for the specimens without nucleating agent). Table 1 summarises the DTA results and Table 2 shows the crystallisation products after heat treating the samples at their respective DTA exo-peak temperatures for the indicated time periods. It must be mentioned that all specimens except specimen B were subjected to a two-stage heat treatment schedule (nucleation and growth). The nucleation temperature (526 °C) was chosen half-way between T_g and T_d temperatures.

From XRD results it was concluded that all specimens show nearly equal amounts of barium hexaferrite phase whereas in

Table 2
Heat treatmet conditions and crystallisation products

Sample	Heat treatment temperature (°C) and time (h)	Crystallisation products
A	As cast (without heat treatment)	Glassy
B	721, (1)	$BF_{(S)}$, $BB_{(VW)}$
C	526, (1) and 721, (1)	$BF_{(S)}$, $BB_{(w)}$
D	526, (3) and 721, (1)	$BF_{(S)}$, $BB_{(M)}$
E	526, (5) and 721, (1)	$BF_{(S)}$, $BB_{(M)}$
F	526, (1) and 721, (5)	$BF_{(S)}$, $BB_{(W)}$
G	526, (2) and 721, (5)	$BF_{(S)}$, $BB_{(M)}$
H	526, (3) and 721, (5)	$BF_{(S)}$, $BB_{(VS)}$
I	526, (5) and 721, (5)	$BF_{(S)}$, $BB_{(VS)}$

X-ray diffraction intensities are written in parantheses. VW, very weak; w, weak; M, moderate; S, strong; VS, very strong.

the case of BaB_2O_4 (BB) phase it seems that nucleation step facilitates its crystallization process (compare specimens B and D) and longer nucleation and growth times (a longer than 3 h nucleation, followed by a 5 h growth step) greatly enhances the quantity of the latter phase. This can be explained by the relatively weak tendency of BB phase for bulk nucleation in these glasses, necessitating longer nucleation periods (as previously stated in refs. [14,15]) and also by the increased viscosity of glass specimens due to the addition of ZrO_2. It is also interesting to note that the amounts of BB phase were much smaller in these specimens in comparison to similar glass compositions without the ZrO_2 additive and subjected to similar heat treatment operations.

3.2. Microstructurul investigations

Fig. 2 represents a SEM micrograph of specimen A. It is obvious that this glass has been phase separated prior to any heat treatment process. As proved by EDS analysis, the droplet phase is richer in Fe_2O_3 and BaO. Consdering the higher T_g and T_d tempetures of ZrO_2 containing specimens in comparison to the specimens lacking this oxide (Table 1) it also can be postulated that the continuous matrix phase has a higher viscosity, probably owing to a more interconnected glass network structure. In addition to SiO_2, B_2O_3 and Fe_2O_3 oxides in the presence of sufficient amounts of BaO, as oxygen donor, can also gain four-fold coordination and take part in the interconnected glass network.

Fig. 3 represents a SEM micrograph of specimen B. It can be seen that this specimen exhibited a quite non-uniform microstructure regarding the size and shape of crystallised particles. Some particles with regular hexagonal shape have grown to quite big sizes, whereas other particles situated between the phase separated droplets exhibited very fine needle like morphology and the platelets grown within the phase separated droplet phases were of larger sizes. All these particles are $BaFe_{12}O_{19}$ as proved by energy dispersive spectroscopy (EDS) and XRD.

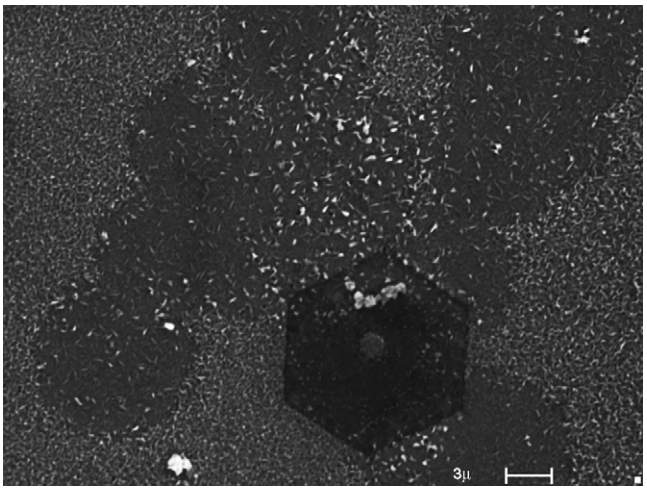

Fig. 3. SEM micrograph of specimen B, showing several varieties of $BaFe_{12}O_{19}$ particles, formed after a single stage heat treatment, 1 h at 721 °C.

Table 3
Magnetic properties obtained under a maximum magnetic field of 20 kOe

Specimen	M_s (emu g^{-1})	H_c (Oe)
A	4	100
B	25	2700
C	25.4	2200
D	24	3000
E	26	1900
F	23	2200
G	27	2500
H	29	1800

The well grown hexagonal particles can be attributed to the growth of some pre-existing nuclei or even small crystallites formed during quenching of the glass specimens. The presence of these particles though undetectable by XRD, later proved by SEM and magnetic measurements (see Table 3).

Figs. 4 and 5 represent SEM microstructures of specimen C, nucleated and grown for 1 h at 526 and 721 °C, respectively.

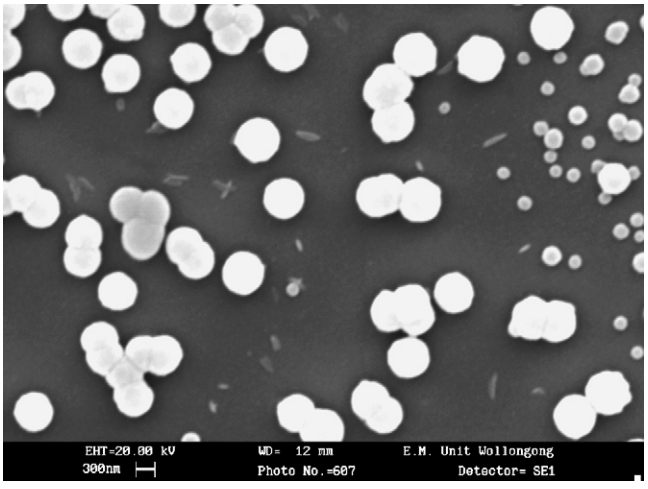

Fig. 2. SEM micrograph of specimen A, showing extensive phase separation in as received glass.

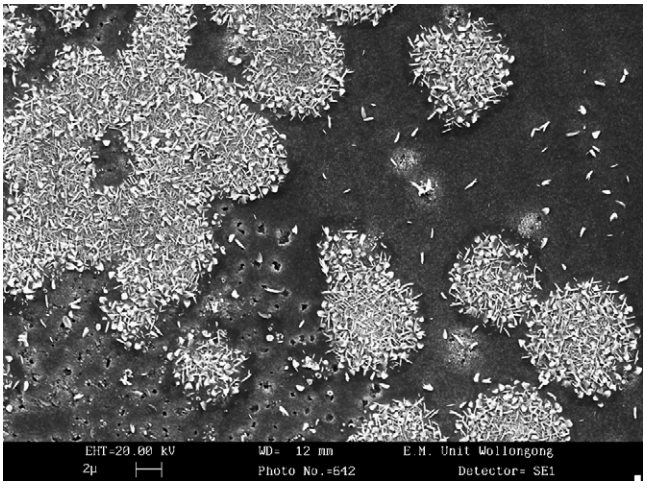

Fig. 4. SEM micrograph of specimen C, showing crystallization of $BaFe_{12}O_{19}$ Particles initiated within the droplet phase.

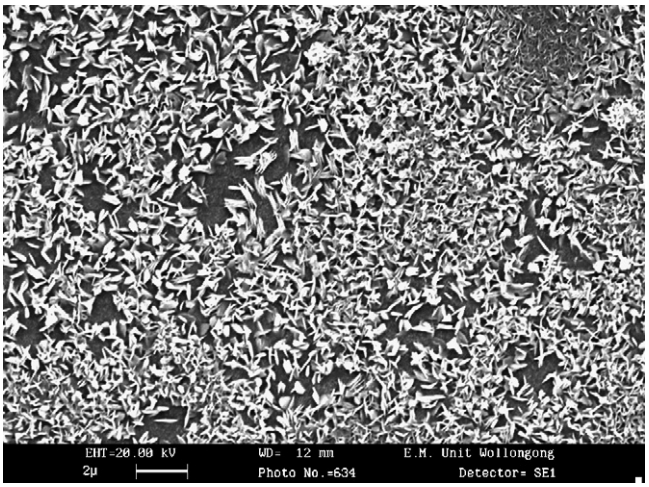

Fig. 5. SEM micrograph of specimen C, showing the distribution of crystallized platelets in the microstructure. *Note*: The difference in size between particles crystallized inside and outside the droplet regions.

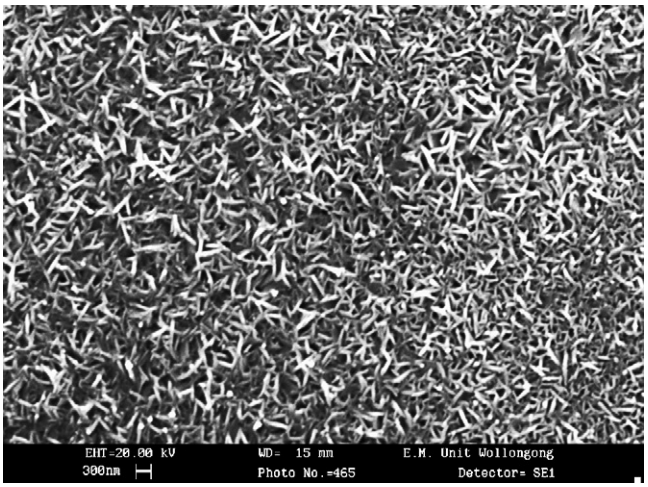

Fig. 7. SEM micrograph of specimen D showing a uniform structure consisting of fine platelets.

It can be seen that the crystallisation of barium hexaferrite particles has initiated from the interior of droplet phases. This can be explained by reduced viscosity of the glass phase in these regions, leading to higher mobility of ions and also by its enrichment by Fe_2O_3 (Fig. 6), increasing the crystallisation driving force (corresponding to the free energy difference $|\Delta G_c|$ between the partially crystallised glass ceramic and the supercooled melt). Such glass composition changes towards the composition of the crystallising phase is well known to raise $|\Delta G_c|$ [19]. Fig. 7 depicts a SEM microstructure of specimen D, nucleated at 526 °C for 3 h and grown at 721 °C for 1 h. Longer nucleation period of these specimens, has led to a finer and more uniform microstructure of platelet particles.

It seems that during this prolonged nucleation period, some particles situated within the intra-droplet regions also have nucleated and grown and joined to the inter-droplet particles. The overall microstructure though exhibiting a relatively uniform picture, but still reveals some microstructural differences regading the size of platelet particles (Fig. 8).

Fig. 9 exhibits SEM microstructure of specimen E nucleated at 526 °C for 5 h and grown at 721 °C for 1 h. It seems that too prolonged nucleation at 526 °C has led to an obviously dual microstructure consisting of very fine particles mainly situated

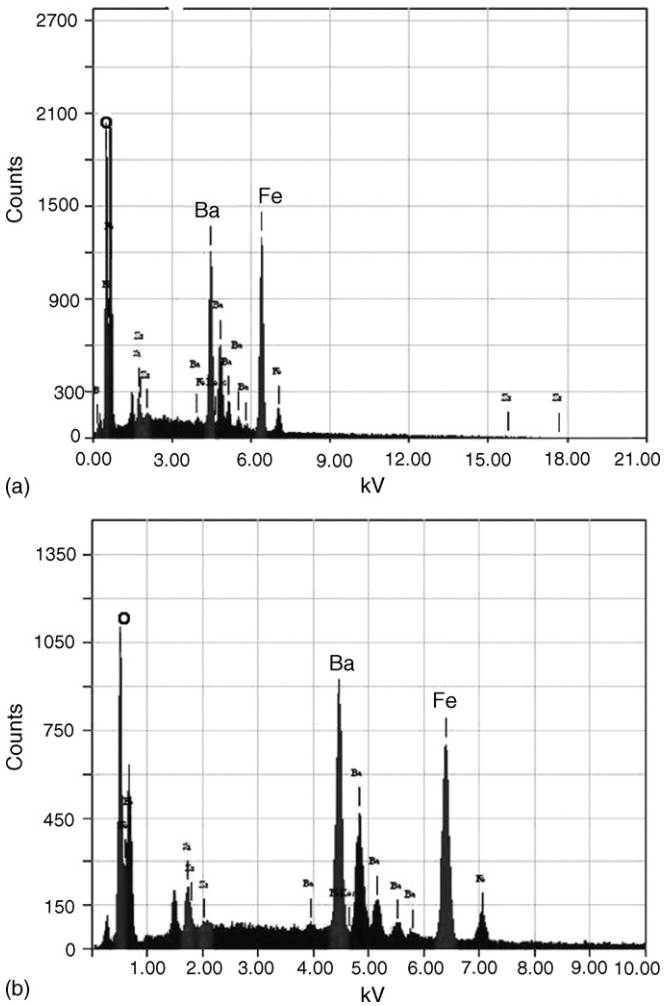

Fig. 6. EDS spectra for phase separated glass A. (a) Inter-droplet and (b) intra-droplet (matrix) phase analysis.

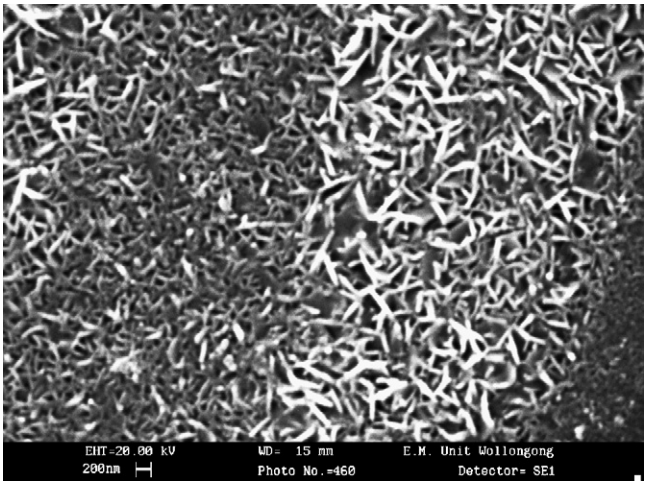

Fig. 8. SEM micrograph of specimen D showing the size difference of particles situated in inter- and intra-droplet regions.

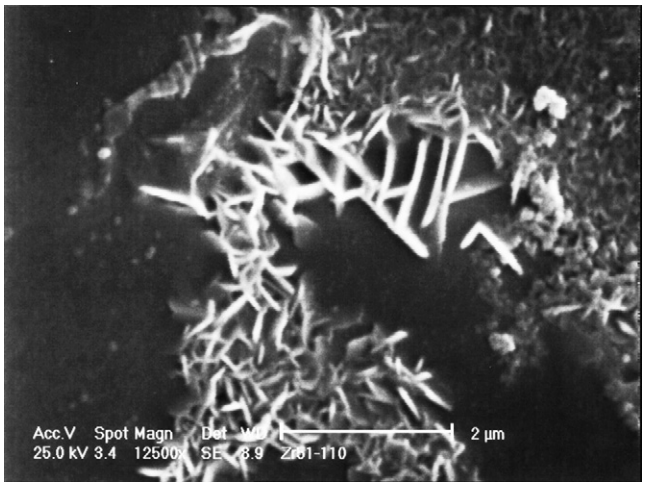

Fig. 9. SEM micrograph of specimen E, showing the tiny particles, crystallized inside the droplet phase and relatively large particles formed in the intra-droplet region.

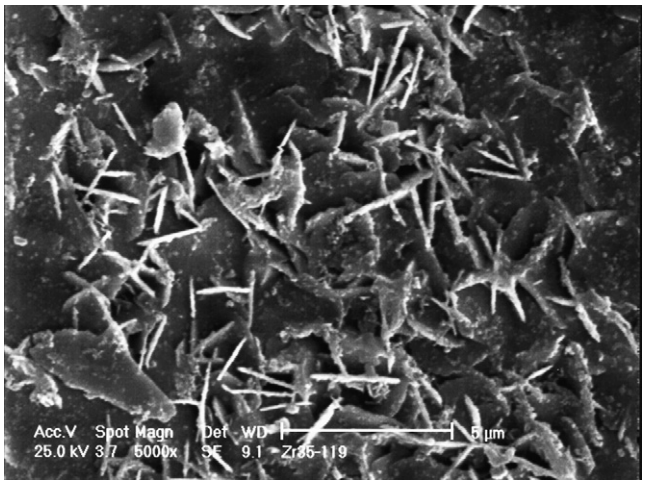

Fig. 11. SEM micrograph of specimen H, depicting the relatively uniform distribution of large particles in the microstructure.

within the droplet regions and some well grown particles located outside these regions.

Fig. 10 shows the SEM microstructure of specimens F nucleated at 526 °C for 1 h and grown at 721 °C for 5 h. It seems that in this specimen the nucleation time has not been sufficiently long to bring about considerable nucleation within the intra-doplet phase and the long growth time has led to a strongly nonuiform structure. In the case of specimen H on the other hand the relatively prolonged nucleation period of 3 h has apparently resulted in a more or less uniform but relatively coarser structure (Fig. 11).

3.3. Magnetic properties

Table 3 summarises the magnetic properties of prepared specimens. It can be seen that the specimens show saturation magnetisation values in the range of 23–29 emu/g.

Considering the fact that the content of iron oxide determines the amount of $BaFe_{12}O_{19}$ phase, it can be estimated that the maximum amount of possible ferrite phase in these compositions is theoretically ∼50 wt%. It has been reported [20] that the theoretical value of M_s for barium hexaferrite single crystal is 72 emu/g. Therefore, it can be concluded that the measured M_s values in this experiment are in the range of 64–80% the theoretical value.

In contrast to the M_s values, the H_c values obtained in this work greatly differ for various specimens. The coercivity values (H_c) in addition to crystal structure mainly depend on the size and shape of the particles of magnetic phase. Finer particles and specific shapes usually increase the value of H_c [3,5,8,12]. The variation of H_c values in specimens C–E with a constant growth time of 1 h at 721 °C, while the nucleation time varied in 1–5 h range, can be explained as follows: in specimen C the insufficient nucleation time of 1 h resulted in relatively small particles with a mean size of ∼480 nm originated from inter-droplet regions and mostly large particles from intra-droplet regions with a mean size of 1.2 μm giving rise to a moderate value of H_c = 2200 Oe, wherease in specimen D the longer nucleation time, giving an opportunity for more efficient nucleation within the intra-droplet regions, resulted in a more uniform and fine microstructure.

This microstructure consisting of tiny platelets of ∼420 nm mean size originated from inter-droplet regions (which are the majority of particles) along with some larger particles with a mean size of ∼600 nm from intra-droplet regions was responsible for the relatively high value of H_c = 3000 Oe. It is well known that the critical size of barium hexaferrite particles below which the particles may magnetically be single domain is 460 nm [12,21]. Single domain particles may have a marked effect in increasing H_c values, while multi-domain particles usually reduce H_c. In multi-domain particles the processes of magnetisation and demagnetisation proceed by the relatively easy process of domain wall motion, whereas in single domain particles (in which formation of domain walls is energetically unfavourable owing to very small sizes of particles) the magnetisation and demagnetisation proceed by the difficult process of rotation of magnetisation vector [1].

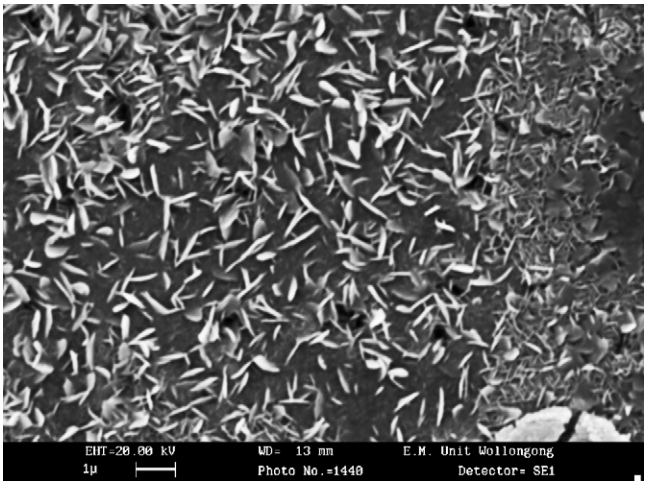

Fig. 10. SEM micrograph of specimen F, showing the difference in size between crystallized particles, located insde or outside the droplet phase.

It may be suggested that in specimen D most of the particles located in the droplet phase were single domain (which were the majority of the particles) wherease some of the particles sutuated in intra-droplet regions were multidomain.

By increasing the nucleation time to 5 h (specimen E) a distinctly bimodal distribution of particles resulated, consisting of numerous tiny and superparamagnetic particles situated within the inter-droplet regions and many multidomain particles originated from intra-droplet regions (Fig. 9). This microstructure resulted in a quite reduced value of H_c = 1900 Oe.

Regarding the specimens F and H with a constant growth time of 5 h and nucleation times varying in 1–3 h range, the following conclusions may be drawn: in specimen F, the relatively short nucleation and long growth times which resulted in a dual and strongly non-uniform microstructure, as described before (Fig. 10), gave a moderate value of H_c = 2200 Oe. On the other hand in specimen H, exhibiting the lowest value of H_c = 1800 Oe, the longer nucleation time has resulted in a more uniform, though well grown microstructure, with a mean size of 1.8 μm for particles which were mostly multi-domain (Fig. 11).

Finally specimen B that as a result of the absence of nucleation step in its heat treatment schedule, exibited the most non-uniform microstructure regarding the size and shape of Ba-hexaferrite particles (Fig. 3), showed a relatively higher conercivity value of H_c = 2700 Oe. This was the result of more complicated interactions of numerous particles of different shapes and sizes ranging from tens of nanometers to well grown hexagonal particles of tens of micrometers.

4. Conclusions

Formation of amorphous ribbons of composition 0.35 BaO·0.35 Fe_2O_3·0.20 B_2O_3·0.10 SiO_2 with addition of 1% ZrO_2 as a nucleant, and their subsequent crystallisation were investigated. DTA results revealed the existence of a marked tendency towards bulk crystallisation.

It was proved that the nucleation heat treatment has a profound effect on the microstructure and magnetic properties of specimens.

At a constant nucleation heat treatment temperature of 526 °C there exists an optimum time for nucleation leading to the highest H_c values.

This can be explained by considering the microstructure of glass specimens, which are strongly phase separated exhibitng spherical Fe-rich droplets dispersed in a matrix phase. In shorter or longer nucleation times the existing difference between inter- and intra-droplet nucleation rates gives rise to a bimodal distribution of small Ba-hexaferrite crystallites situated in the inter-droplet and larger particles in the intra-droplet regions. Whereas for an optimum nucleation time, the relative balance achieved between the concentration of nuclei in two regions, gives rise to a relatively uniform distribution of fine particles.

It was proved that the growth time is also important in controlling the crystal mean size of the final microstructures, and it should be kept at a necessary minimum.

In the present work a 3 h nucleation at 526 °C following by 1 h hold at 721 °C for growth, gives a uniform microstructure of fine particles and a coercivity value of H_c = 3000 Oe, which is the highest amongst the specimens investigated herein.

All specimens developed $BaFe_{12}O_{19}$ and BaB_2O_4 as the only crystalline phases, the latter being a minor phase except in specimens heat treated at 526 °C for ≥3 h and 721 °C for 5 h.

The values of saturation magnetisation (M_s) were varied in 23–29 emu/g range, the maximum amount observed in specimens subjected to an optimum nucleation time (3 h) following by a prolonged growth time (5 h). The latter specimens showed the minimum value of H_c = 1800 Oe owing to their relatively large crystal sizes.

Acknowledgments

The authors would like to acknowledge the financial support of this research work by Iran Ministry of Science, Research and Technology and Iran University of Science and Technology. We also thank Dr. A.V. Pan and S. Keshavarzi from Institute of Superconducting and Electronic Materials and M. Ahmadian from School of Materials and Mechanical Engineering, Wollongong University, Australia for their kind cooperation and technical help and M. Kord and A. Bahrami from Iran University of Science and Technology for their valuable assistance in preparation of specimens.

References

[1] B.T. Shirk, W.R. Buessem, Magnetic properties of barium ferrite formed by crystallisation of glass, J. Am. Ceram. Soc. 53 (1970) 192–196.
[2] O. Kubo, T. Ido, H. Yocoyama, Properties of barium ferrite particles for perpendicular magnetic recording medias, IEEE Trans. Magn. Mag-18 (1982) 1122–1124.
[3] K. Oda, T. Yoshio, K.O. Oka, Morphology and magnetic properties of $BaFe_{12}O_{19}$ particles prepared by the glass-ceramic method, J. Mater. Sci. Lett. 20 (1985) 876–879.
[4] H. Zagnazi, C. Chaumont, J.C. Bernier, Rules for the preparation of powders by the glass synthesis method—application to barium hexaferrite, J. Solid State Chem. 65 (1986) 370–376.
[5] S. Ram, D. Bahadur, D. Chakravorty, Magnetic glass-ceramics with hexagonal lead ferrites, J. Non-cryst. Solids 88 (1986) 311–322.
[6] F. Haberey, Propartion of M and W-type hexaferrite particles by the glass crystallisation method on the basis of the pseudo-ternary system Fe_2O_3–BaO–B_2O_3, IEEE Trans. Magn. Mag-23 (1987) 29–32.
[7] S. Ram, D. Bahadur, D. Chakravorty, Crystallisation of W-type hexagonal ferrites in an oxide glass with As_2O_3 as nucleation catalyst, J. Magn. Mater. 67 (1987) 378–386.
[8] P. Brahma, K. Choudhury, R. Guha, D. Chakravorty, Crystallisation of Ba-M ferrite in a glass with Sb_2O_3 as nucleation catalyst, J. Mater. Sci. Lett. 24 (1989) 540–542.
[9] C.K. Lee, R.F. Speyer, Glass formation and crystallisation of barium ferrite in the Na_2O–BaO–Fe_2O_3–SiO_2 system, J. Mater. Sci 29 (1994) 1348–1351.
[10] C.K. Lee, R.F. Berta, R.F. Speyer, Effect of Na_2O addition in the crystallisation of barium ferrite from a BaO–B_2O_3–Fe_2O_3 glass, J. Am. Ceram. Soc. 79 (1996) 183–192.
[11] K. Watananabe, K. Hoshi, Crystallisation kinetics of fine barium hexaferrite, $BaFe_{12}O_{19}$ particles in a glass matrix, Phys. Chem. Glasses 40 (1999) 75–78.
[12] L. Rezlescu, E. Rezlescu, P.D. Popa, N. Rezlescu, Fine barium hexaferrite powder prepared by the crystallisation of glass, J. Magn. Magn. Mater. 193 (1999) 288–290.

[13] V.K. Marghussian, A. Beitollahi, M. Haghi, The effect of SiO_2 and Cr_2O_3 additions on the crystallisation behaviour and magnetic properties of a B_2O_3–BaO–Fe_2O_3 glass, Ceram. Int. 29 (2003) 455–462.
[14] M. Mirkazemi, V.K. Marghussian, A. Beitollahi, Microstructure and magnetic properties of BaO–Fe_2O_3–B_2O_3–SiO_2 glass ceramics, Ceram. Int. 32 (2006) 43–51.
[15] M. Mirkazemi, A. Beitollahi, V.K. Marghussian, Microstructure and magnetic properties of BaO–Fe_2O_3–B_2O_3–SiO_2 glass ceramics with ZrO_2 as nucleating agent, Phys. Stat. Sol. (C)1 (12) (2004) 3216–3226.
[16] S.B. Sohn, S.Y. Choi, I.B. Shim, Preparation of Ba-ferrite containing glass-ceramics in BaO–Fe_2O_3–SiO_2, J. Magn. Magn. Mater. 239 (2002) 533–536.
[17] P. Görnert, E. Sinn, W. Schüppel, H. Pfeiffer, M. Rösler, Th. Schubert, M. Jurisch, R. Selger, Structural and magnetic propertis Of $BaFe_{12-2x}Co_xTi_xO_{19}$ powder prepared by the glass crystallisation method, IEEE Trans. Magn. 26 (1990) 12–15.
[18] H. Zagnazi, M. Malassis, C. Chaumont, J.C. Bernier, Praparation of cobalt and Fluorine-doped barium hexaferrite by the glass synthesis method, J. Am. Ceram. Soc. 73 (1990) 167–169.
[19] P.F. James, Nucleation and crystallisation in glasses, in: J.H. Simmons, D.R. Uhlmann, G.H. Beall (Eds.), Advances in Ceramics, vol. 4, Am. Ceram. Soc., 1982, p. 1.
[20] S. Ram, D. Chakravorty, D. Bahadur, Effect of nucleating agents on the crystallisation behaviour of barium hexaferrite in a borate glass, J. Magn. Magn. Mater. 62 (1986) 221–232.
[21] B.T. Shirk, W.R. Buessem, Temperature dependence of M_s and k_1 of $BaFe_{12}O_{19}$ and $SrFe_{12}O_{19}$ single crystals, J. Appl. Phys. 40 (1969) 1294–1296.